Earth and Planetary Science Letters 432 (2015) 223–231

Contents lists available at ScienceDirect

Earth and Planetary Science Letters

www.elsevier.com/locate/epsl

# Extending the Cantabrian Orocline to two continents (from Gondwana to Laurussia). Paleomagnetism from South Ireland

Daniel Pastor-Galán[a,*], Bart Ursem[a], Patrick A. Meere[b], Cor Langereis[a]

[a] Paleomagnetic Laboratory "Fort Hoofddijk", University of Utrecht, Budapestlaan 17, 3584CD, Utrecht, The Netherlands
[b] School of Biological, Earth & Environmental Sciences, University College Cork, Cork, Ireland

ARTICLE INFO

*Article history:*
Received 30 July 2015
Received in revised form 17 September 2015
Accepted 11 October 2015
Available online xxxx
Editor: A. Yin

*Keywords:*
tectonics
Variscan
Pangea
Orocline
paleomagnetism
vertical axis rotation

ABSTRACT

Regional Variscan structure in southern Ireland follows a gentle arcuate trend of ca. 25° concave to the SE that apparently follows the geometry of the Cantabrian Orocline (NW Iberia) when Iberia is restored to its position prior to the opening of the Biscay Bay. We report paleomagnetic results from Devonian and Carboniferous rocks in southern Ireland: (i) a pervasive and consistent remagnetization during the Late Carboniferous and (ii) an average rotation of ∼25° counterclockwise with respect to the Global Apparent Polar Wander Path and kinematically compatible with the Cantabrian Orocline. These results support the participation of Laurussia in the formation of the Cantabrian Orocline involving, at least, southern Ireland and the South Portuguese Zone (S Iberia). We conclude that a Greater Cantabrian Orocline extends beyond its current boundaries to include shear zones in the Variscan hinterland and the Rheic Ocean suture, thereby enlarging its size to plate-scale affecting as it does the Laurussia and Gondwana margins.


## 1. Introduction

Earth's history has been dominated by cycles of continent assembly and breakup. Tectonic and paleogeographic reconstructions are critical for understanding orogenic processes, crustal growth and global geodynamics and the associated development of topographic relief as well as natural resources or hazards. Most tectonic restorations consider plates as fully rigid bodies that wander across the Earth's surface following the basic principles of plate tectonics (e.g. Stampfli et al., 2013; Domeier and Torsvik, 2014). In contrast, orocline formation is a process in which roughly linear continents or segments of continent bend into a curved configuration. Oroclines are widespread in space and time (Johnston et al., 2013; Rosenbaum, 2014), present curvatures ranging from a few degrees to as much as 180° (Johnston, 2001; Allmendinger et al., 2005), may affect the entire lithosphere (Pastor-Galán et al., 2012) and may represent up to thousand kilometers of shortening (Weil et al., 2013; Shaw et al., 2012, 2014). Identifying oroclines and unraveling their kinematics is essential to provide accurate tectonic and paleogeographic reconstructions.

The assembly of the supercontinent Pangea was the result of the Late Paleozoic collision between Gondwana, Laurussia (Laurentia + Baltica + Avalonian terranes) and several microplates during the Variscan–Alleghanian orogen (Nance et al., 2010). This orogen shows several striking bends and among them, the Cantabrian Orocline stands out as probably the best studied orocline on Earth (Gutiérrez-Alonso et al., 2012; Weil et al., 2013). Extensive paleomagnetic and structural data constrain the Cantabrian Orocline development from Moscovian to Asselian times (∼310–295 Ma. Weil et al., 2010; Pastor-Galán et al., 2011, 2014, 2015). Its formation led to coeval lithospheric delamination and consequent widespread magmatism (Gutiérrez-Alonso et al., 2011a, 2011b). The kinematics of the Cantabrian Orocline (Weil et al., 2013; Pastor-Galán et al., 2015) require significant amounts of shortening and extension (Pastor-Galán et al., 2012) yet to be included in global reconstructions.

During the amalgamation of Pangea Ireland was part of the Laurussian continent (Nance et al., 2010). The Variscan belt in southern Ireland shows approximately 25° of curvature concave to the SE that could be the continuation of Cantabrian Orocline, once Iberia is restored to a pre-Cretaceous stage (Fig. 1). The origin of this curvature, its kinematics and the prospective linkage with the Cantabrian Orocline is unknown. The hypothesis of a Greater Cantabrian Orocline involving parts of Laurussia would increase the required shortening and extension rates (over 10 cm/yr) creating larger space problems into the reconstructions of Pangea. In this paper we use paleomagnetism to investigate the kinematics of the curvature in the southern Irish Variscides and their possible relation with the Cantabrian Orocline.

* Corresponding author.
*E-mail address:* D.PastorGalan@uu.nl (D. Pastor-Galán).

http://dx.doi.org/10.1016/j.epsl.2015.10.019
0012-821X/

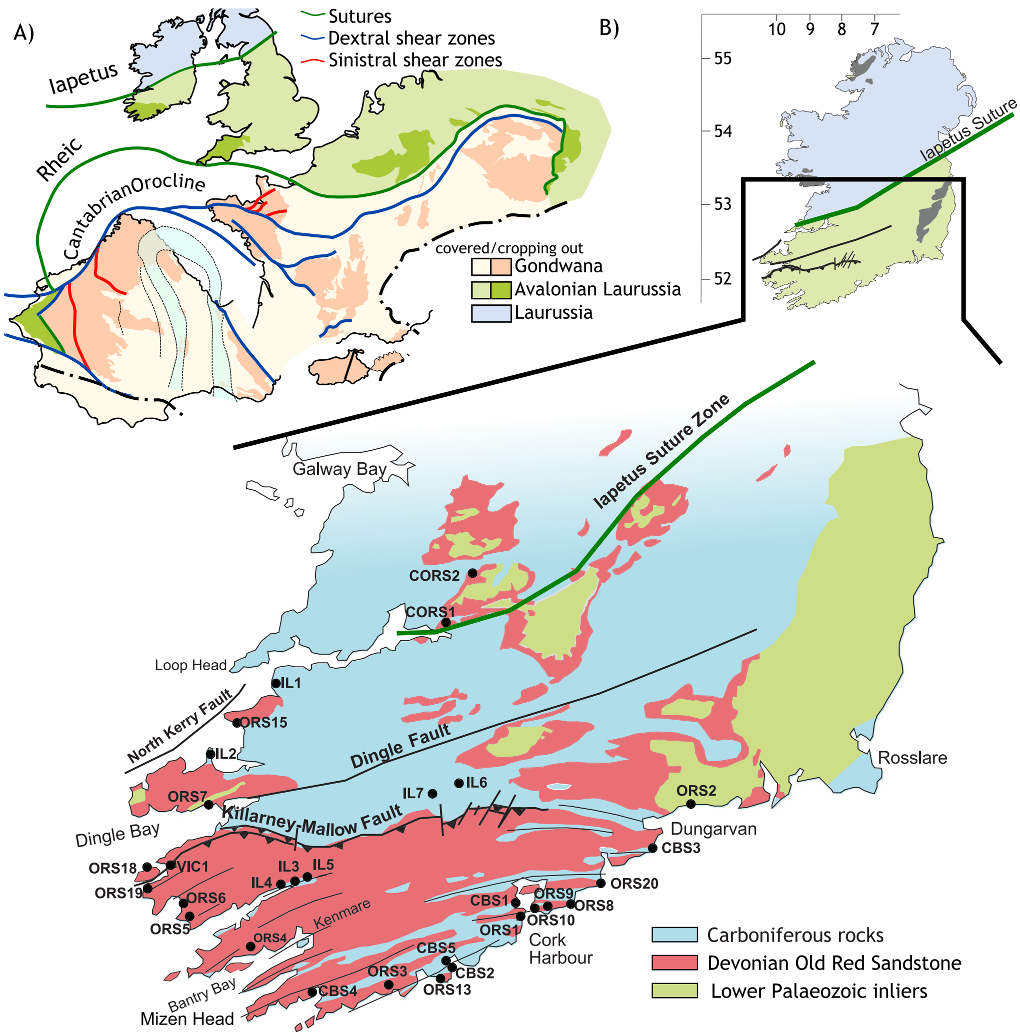


**Fig. 1.** A) The Variscan Orogen of Western Europe, showing the Rheic and Iapetus sutures and the Gondwana and Laurussia affinities, and the trace of the Cantabrian Orocline. B) Simplified geological map of South Ireland, showing major structures and location of samples.

## 2. Geological background

### 2.1. Tectonic history

During the Ediacaran, the constitutive pieces of Gondwana were separated from the northern continental masses, Laurentia and Baltica, by the Iapetus and Tornquist oceans. A protracted period of rifting in the Cambrian led to the opening of the Rheic Ocean in the Early Ordovician and the consequent separation of several micro-continents from the Gondwana margin (Nance et al., 2010; Fernández-Suárez et al., 2014), known as Avalonia *sensu lato* (including among others Avalonia *s.s.*, Ganderia, Carolinia, Meguma...). It is still not clear if the Rheic ocean opened due to slab-pull after Iapetus ridge subduction, slab roll-back underneath Gondwana or both (Pastor-Galán et al., 2013a). Throughout the Ordovician and Silurian the Iapetus and Tornquist oceans were consumed as Avalonia drifted northward towards Baltica and Laurentia culminating in the amalgamation of all three landmasses during the Late Silurian–Early Devonian and creating the Appalachian–Caledonide orogen in the process (Mac Niocaill, 2000; Torsvik et al., 2012). At that time the Rheic Ocean had reached its greatest width (ca. 4000 km; Nance et al., 2010). The onset of closure of the Rheic Ocean began in the Early Devonian. The polarities of subduction zones are highly disputed and include subduction towards Laurussia, Gondwana or both (Stampfli et al., 2013; Pastor-Galán et al., 2013b; Domeier and Torsvik, 2014 and references therein). The Rheic ocean was totally consumed by the Mississippian following the Gondwana and Laurussia collision which formed the Variscan–Alleghanian–Ouachita belt that sutured Gondwana and Laurussia to form Pangea (Nance et al., 2010).

The Cantabrian Orocline of NW Iberia is a large scale orogenic bend that developed just after the development of the Variscan orogen in Iberia, from 310 to 295 Ma (Pastor-Galán et al., 2011, 2014; Weil et al., 2013). Gutiérrez-Alonso et al. (2011a, 2011b) propose a thick-skinned model for oroclinal development which involves lithospheric-scale rotation of the orogen limbs, with extension in the outer arc resulting in thinning of the mantle lithosphere, and coeval shortening in the inner arc (Pastor-Galán et al., 2012) and subsequent lithospheric delamination (Gutiérrez-Alonso et al., 2011a, 2011b). Although the kinematics of the Cantabrian Orocline are well known, there is still a debate about the plausible geodynamic mechanisms and tectonic scenarios responsible for the buckling (Weil et al., 2013 and references therein).

### 2.2. Regional background

Southern Ireland lies at the northern margin of Avalonian terranes afected by the European Variscan orogeny. The geology of southern Ireland is dominated by the terrigenous siliciclastic fill of the Late Silurian–Devonian basins, traditionally known as Old Red Sandstone [ORS hereafter] (Williams, 2000). Over seven kilometers of Upper Devonian ORS sediment accumulated in the depocentre of the largest basin, the Munster Basin (MacCarthy, 1990). Lithologically the ORS mainly consists of fine-grained sandstones and siltstones with a number of relatively minor conglomeratic units primarily restricted to the east basin margin (MacCarthy, 1990). The end of the Devonian marks the onset of a regional marine transgression with the development of a sub-basin, the South Munster Basin to the south (MacCarthy, 1990; Williams et al., 1989). Extensional tectonic activity in southern Ireland ceased with the Late Carboniferous onset of Variscan compressional tectonics.

The style of deformation in South Ireland was strongly controlled by the position of pre-existing basin-bounding faults and basin geometry (Price and Todd, 1988; Meere, 1995). The regional structural grain (cleavage, fold axes) follows a gentle, very smooth and continuous arcuate trend of ca. 25° with an ENE–WSW strike in the west swinging into a more E–W strike in the east (Fig. 1B). Overall, deformation involved dominantly pure shear, thick skinned, basin inversion with no evidence of low angle thrust faulting or localized block rotations typical of a classic fold/thrust belt. Deformation south of the Killarney–Mallow Fault (Fig. 1) is characterized by large-scale open to closed periclinal regional folds, an intense pervasive axial planar cleavage fabric, reactivation of high angle basin controlling normal faults and a late-stage phase of brittle deformation (Price and Todd, 1988; Meere, 1995; Quinn et al., 2005). To the north of this strain boundary deformation is characterized by gentle folds and locally developed disjunctive axial planar cleavage. The axial traces of folds in this zone tend to follow a more NE–SW inherited Caledonian trend.

## 3. Data acquisition and results

We drilled a total of 229 cores with a petrol engine drill we collected 25 oriented hand samples in 30 different sites (Fig. 1b; Table 1; Supplementary material for exact location) including Devonian Sandstones (19 sites with codes ORS, CORS and VIC), Mississippian Sandstones (4 sites, code CBS) and Pennsylvanian Limestones (7 sites, code IL).

Magnetic remanence of samples was investigated through thermal and alternating field (AF) demagnetization. AF demagnetization was carried out using a robotic 2G-SQUID magnetometer, through variable field increments (4–10 mT) up to 70–100 mT. In those samples where high-coercivity, low-blocking temperature minerals (e.g. goethite, maghemite) were expected, a pre-heating to 150 °C was coupled to AF demagnetization. Stepwise thermal demagnetization was carried through 20–100 °C increments up to complete demagnetization in the rest. Principal component analysis (Kirschvink, 1980; Ramón and Pueyo, 2012) was used to calculate magnetic component directions from "Zijderveld" vector end-point demagnetization diagrams. Representative Zijderveld diagrams are shown in Fig. 2.

Mean directions (Table 1) were evaluated using Fisher statistics of virtual geomagnetic poles (VGPs) corresponding to the isolated directions (ChRM). Here, the N-dependent A95 envelope of Deenen et al. (2011) was applied to assess the quality and reliability of the ChRM distributions. These criteria assess whether (i) the scatter of virtual geomagnetic poles (VGP) can be straightforwardly explained by paleosecular variation (PSV) of the geomagnetic field ($A95_{min} \leq A95 \leq A95_{max}$), (ii) an additional source of scatter ($A95 > A95_{max}$) is present besides PSV (e.g. structural problems, rotations...), or (iii) the scatter underrepresents PSV, which may indicate acquisition of the magnetization in a time period too short to fully sample PSV, e.g. due to remagnetization or inappropriate sampling. We applied a fixed 45° cut-off to the VGP distributions of each site. Table 1 summarizes the results from Old Red Sandsone (ORS, CORS and VIC), Mississippian sandstones (CBS) and Pennsylvanian limestones (IL). Results show single polarity (reversed) declinations ranging from 186° to 255° and inclinations from −36° to 20°. Site CORS2 yielded no interpretable results.

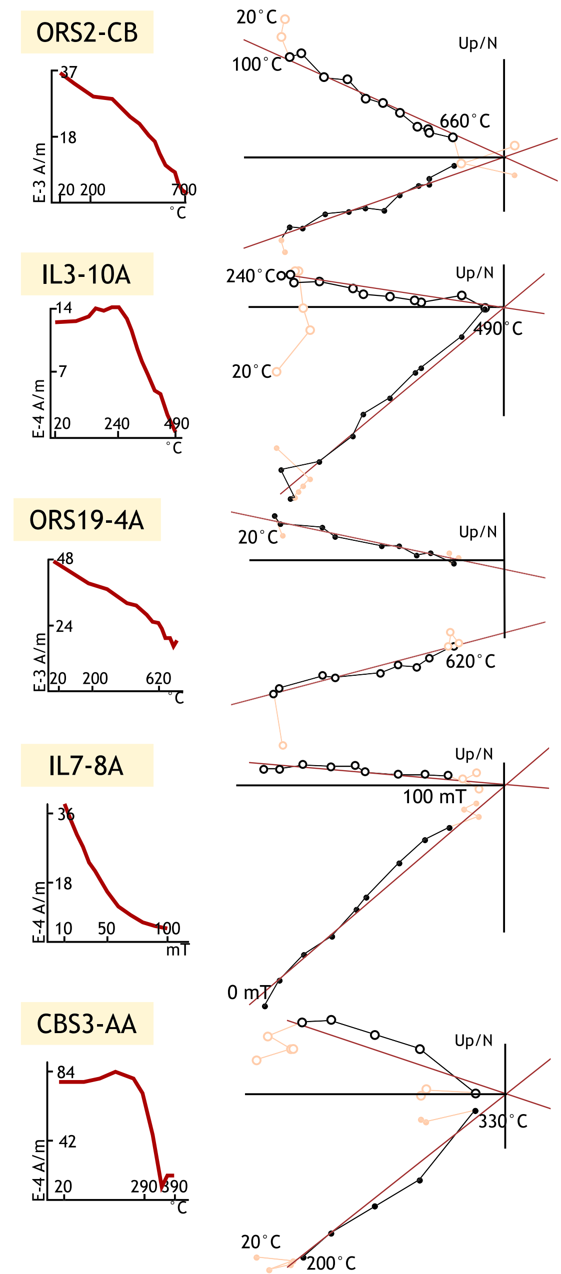


**Fig. 2.** Orthogonal vector diagrams (Zijderveld, 1967), showing characteristic demagnetization diagrams for representative samples from ORS, CBS and IL. Closed (open) circles indicate the projection on the horizontal (vertical) plane. Alternating field (°C) and thermal (mT) demagnetization steps are indicated. All diagrams are in a geographic reference frame.

In many samples a viscous magnetic component is removed at low temperatures (100–180 °C; Fig. 2 and Supplementary material). Occasionally, this viscous component fits with the present-day field. The demagnetization analysis indicates that the principal magnetic carrier of the ChRM in ORS samples is hematite (demagnetizing over 600 °C and few to no AF demagnetization). Most ORS samples behave erratically from 660 °C showing transformation of the hematite to magnetite. A little ORS samples did not decay straight to the origin and due to the aforementioned thermal alteration it was not possible to recover any further component. The principle magnetic carrier in CBS and IL samples is (Ti-)magnetite, evidenced by maximum unblocking temperatures of 480–520 °C and alternating magnetic fields of 60–90 mT (Fig. 2).

**Table 1**
Statistical values for all sites collected showing the number of samples interpreted and the ones that pass the 45° fixed cut-off (see text for details).

| Code | *N* (45) | *N* (B) | In situ statistics | | | | | | | | | | Tilt corrected | | 70% corr. | | Strike orogen* | Strike | Dip | Rock age |
|---|---|---|---|---|---|---|---|---|---|---|---|---|---|---|---|---|---|---|---|---|
| | | | *D* | Δ*D* | *I* | Δ*I* | A95 | $A95_{min}$ | $A95_{max}$ | *K* | (*k*) | (a95) | Dec | Inc | Dec | Inc | | | | |
| IL1 | 7 | 7 (2) | 199.6 | ±3.597 | −20.7 | ±6.4 | 3.5 | 5.5 | 24.1 | 292.7 | 115.3 | 5.6 | 198.1 | 5.1 | | | 69 | 266 | 28 | Pennsylvanian |
| IL2 | 10 | 10 (1) | 208.5 | ±4.1 | 19.0 | ±7.5 | 4 | 4.8 | 19.2 | 143.4 | 123.8 | 4.4 | 201.0 | 16.8 | | | 75 | 30 | 23 | Pennsylvanian |
| IL3 | 15 | 15 | 208.1 | ±4.4 | −11.2 | ±8.5 | 4.4 | 4.1 | 14.9 | 78.0 | 56.6 | 5.1 | 246.6 | −35.2 | | | 68 | 62 | 77 | Pennsylvanian |
| IL4 | 11 | 11 | 226.3 | ±13.3 | −36.1 | ±18.4 | 12.5 | 4.6 | 18.1 | 14.4 | 14.1 | 12.6 | 202.9 | 6.9 | | | 68 | 241 | 82 | Pennsylvanian |
| IL5 | 14 | 14 | 214.3 | ±5.8 | −1.4 | ±8.7 | 7 | 4.2 | 15.6 | 45 | 15.4 | 10.5 | 239.4 | 38.7 | | | 68 | 256 | 77 | Pennsylvanian |
| IL6 | 14 | 14 | 227.2 | ±7.4 | −33.9 | ±10.8 | 7 | 4.2 | 15.6 | 32.8 | 30.0 | 7.4 | 219.4 | 20.3 | 214.1 | 4.4 | 74 | 265 | 75 | Pennsylvanian |
| IL7 | 18 | 18 | 202.6 | ±4.9 | 33.1 | ±7.2 | 4.7 | 3.8 | 13.3 | 56.2 | 26.7 | 6.8 | 197.6 | −6.7 | 198.1 | 4.2 | 74 | 86 | 45 | Pennsylvanian |
| CBS1 | 7 | 10 | 199.8 | ±9.5 | 13.1 | ±18.1 | 9.4 | 5.5 | 24.1 | 42.0 | 26.7 | 11.9 | 220.8 | 53.4 | | | 82 | 61 | 54 | Mississippian |
| CBS2 | 10 | 10 | 203.5 | ±4.2 | 5.9 | ±8.2 | 4.2 | 4.8 | 19.2 | 136.1 | 77.3 | 5.5 | 204.5 | −25.9 | | | 84 | 266 | 54 | Mississippian |
| CBS3 | 9 | 10 | 195.4 | ±5.9 | −21.1 | ±10.4 | 5.8 | 5.0 | 20.5 | 80.8 | 56.4 | 6.9 | 199.0 | −45.0 | | | 90 | 90 | 24 | Mississippian |
| CBS4 | 8 | 10 | 215.1 | ±12.0 | 20.4 | ±21.5 | 11.8 | 5.2 | 22.1 | 22.9 | 11.2 | 17.3 | 210.8 | 3.6 | | | 71 | 68 | 26 | Mississippian |
| CORS1 | 9 | 9 | 207.2 | ±7.0 | 5.4 | ±13.9 | 7 | 5.0 | 20.5 | 54.8 | 25.1 | 10.5 | 206.9 | −2.4 | | | 75 | 64 | 6 | Devonian |
| CORS2 | 0 | 10 (1) | – | – | – | – | – | – | – | – | – | – | – | – | – | – | – | 118 | 2 | Devonian |
| ORS1 | 11 | 12 | 221.8 | ±10.0 | 20.9 | ±17.8 | 9.8 | 4.6 | 18.1 | 22.6 | 19.8 | 10.5 | 223.5 | −22.3 | | | 79 | 70 | 79 | Devonian |
| ORS2 | 8 | 8 | 236.0 | ±12.8 | −15.7 | ±24.0 | 12.7 | 5.2 | 22.1 | 20.1 | 14.6 | 15.0 | 222.3 | −1.9 | | | 94 | 233 | 76 | Devonian |
| ORS3 | 12 | 12 | 228.7 | ±8.6 | 13.7 | ±16.3 | 8.5 | 4.4 | 17.1 | 26.8 | 21.1 | 9.7 | 247.1 | 47.6 | | | 73 | 281 | 44 | Devonian |
| ORS4 | 11 | 15 | 216.2 | ±6.7 | −5.4 | ±13.2 | 6.7 | 4.6 | 18.1 | 48.0 | 37.0 | 7.6 | 223.3 | −20.7 | | | 63 | Fold test | | Devonian |
| ORS5 | 11 | 11 | 215.7 | ±8.0 | 7.2 | ±15.8 | 8 | 4.6 | 18.1 | 33.4 | 25.6 | 9.2 | 216.1 | −26.7 | | | 62 | 117 | 34 | Devonian |
| ORS6 | 11 | 11 | 204.5 | ±10.6 | 11.7 | ±20.3 | 10.5 | 4.6 | 18.1 | 19.9 | 10.8 | 14.6 | 202.1 | 5.0 | | | 62 | Fold test | | Devonian |
| ORS7 | 9 | 10 | 206.5 | ±17.0 | 29.0 | ±26.9 | 16.3 | 5.0 | 20.5 | 10.9 | 10.6 | 16.6 | 207.0 | −29.9 | | | 70 | 68 | 76 | Devonian |
| ORS8 | 8 | 8 | 210.5 | ±5.6 | −9.2 | ±11 | 5.6 | 5.2 | 22.1 | 97.8 | 30.5 | 10.2 | 212.8 | 37.1 | | | 86 | 290 | 47 | Devonian |
| ORS9 | 16 | 16 (3) | 211.6 | ±7 | 32.8 | ±14 | 5.6 | 4 | 14.3 | 33.0 | 40.2 | 5.9 | 278 | 48.4 | | | 82 | 255 | 66 | Devonian |
| ORS10 | 10 | 10 (2) | 225.6 | ±9.3 | −12.1 | ±17.9 | 9.3 | 4.8 | 19.2 | 28.2 | 20.4 | 11.0 | 224.3 | 5.7 | | | 77 | 262 | 29 | Devonian |
| ORS13 | 14 | 14 (2) | 199.2 | ±3.2 | 10.7 | ±6.1 | 3.2 | 4.2 | 15.6 | 159.9 | 81.3 | 4.4 | 227.9 | −46.4 | | | 74 | 68 | 86 | Devonian |
| ORS14 | 12 | 13 (4) | 197 | ±7.6 | 2.2 | ±13.1 | 7.5 | 4.4 | 17.1 | 34.9 | 17.6 | 10.6 | 197.7 | −23.9 | | | 71 | 75 | 31 | Devonian |
| ORS15 | 14 | 14 (3) | 217.9 | ±8.5 | −1.5 | ±17.1 | 8.5 | 4.2 | 15.6 | 22.6 | 13.8 | 11.1 | 218.7 | −11.2 | | | 69 | 92 | 12 | Devonian |
| ORS16 | 14 | 14 (2) | 227.5 | ±8.3 | −28.2 | ±13.3 | 8 | 4.2 | 15.6 | 25.7 | 15.2 | 10.5 | 255.5 | −26.7 | | | 73 | 60 | 50 | Devonian |
| ORS18 | 9 | 9 (2) | 223.0 | ±5.2 | −5.3 | ±10.3 | 5.2 | 5.0 | 20.5 | 99.4 | 94.2 | 5.3 | 224.8 | −9.2 | | | 65 | 59 | 15 | Devonian |
| ORS19 | 11 | 11 (1) | 210.8 | ±5.2 | 12.9 | ±10.0 | 5.2 | 4.6 | 18.1 | 77.7 | 34.4 | 7.9 | 207.7 | −2.9 | | | 65 | 53 | 38 | Devonian |
| ORS20 | 9 | 11 | 229.1 | ±13.6 | −0.9 | ±27.2 | 13.6 | 5.0 | 20.5 | 15.2 | 8.6 | 18.6 | 232.7 | −23.7 | | | 85 | 104 | 36 | Devonian |
| VIC1 | 13 | 13 (2) | 203.3 | ±2.2 | −29 | ±3.7 | 2.1 | 4.3 | 16.3 | 376.9 | 326.8 | 2.3 | 200.4 | 24.7 | | | 65 | 235 | 85 | Devonian |
| N-KF** | 108 | 112 | 212.3 | ±3.4 | −1.4 | ±6.9 | 3.4 | 1.8 | 4.3 | 16.7 | 16.7 | 5.1 | | | | | | | | |
| N-KF-TC** | 111 | 112 | 209.2 | ±3 | 1.6 | ±6 | 3 | 1.8 | 4.2 | 21 | 21 | 4 | | | | | | | | |
| S-KF** | 238 | 250 | 213.3 | ±2.2 | −0.9 | ±4.4 | 2.2 | 1.3 | 2.6 | 18 | 18 | 3.1 | | | | | | | | |
| S-KF-TC** | 208 | 251 | 220.3 | ±3.1 | −11 | ±6 | 3.1 | 1.4 | 2.8 | 11.2 | 11.2 | 4.3 | | | | | | | | |
| ALL | 327 | 335 | 212.1 | ±1.9 | 0.5 | ±1.9 | 1.9 | 1.2 | 2.1 | 18.5 | 9.6 | 2.9 | | | | | | | | |
| ALL TC | 294 | 335 | 214.5 | ±2.4 | −5.1 | ±4.8 | 2.4 | 1.2 | 2.3 | 12.5 | 6.8 | 3.4 | | | | | | | | |
| | LATS | 51.9 | LONS | −8.96 | | POLE: | PLAT | 2 | PLONG | 133 | | | | | | | | | | |

* Strike for the orocline test is based on fold axes trend.

** N-KF: Average of all samples collected to the North of Killarney Fault in geographical coordinates and N-KF-TC in tectonic coordinates. S-KF and S-KF-TC average of all samples collected to the South of Killarney Fault in geographic and tilt corrected coordinates respectively.

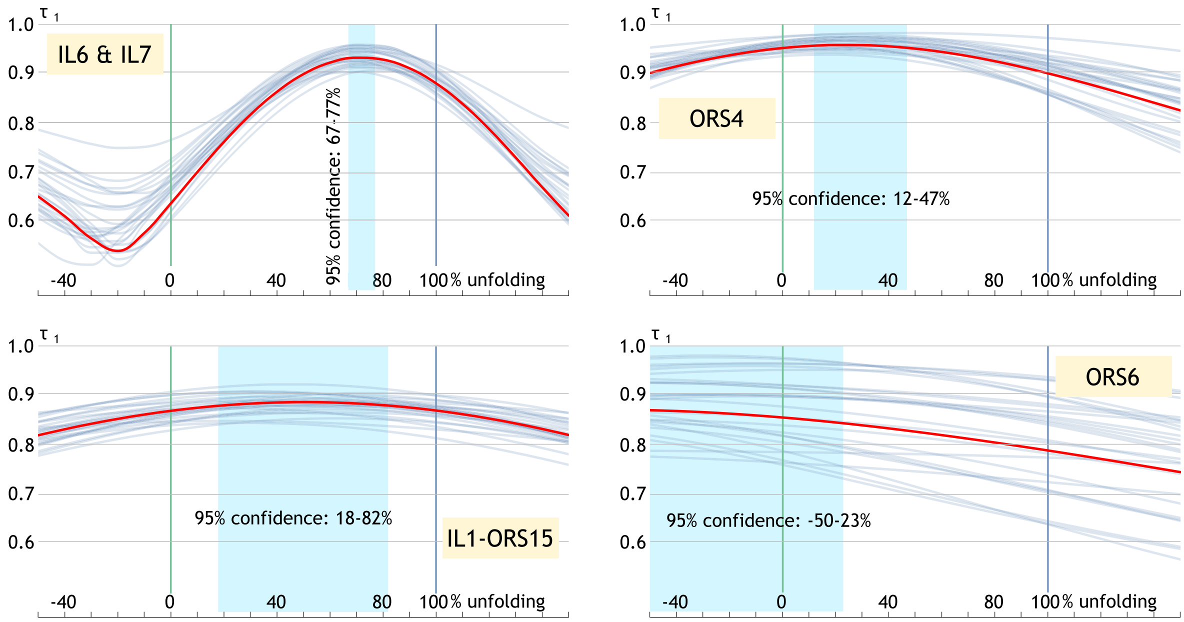


**Fig. 3.** The four performed fold-tests following the methodology of Tauxe and Watson (1994) showing syn-folding (IL6–IL7), and inconclusive magnetizations.

We have performed 4 fold-tests following the Tauxe–Watson method (Tauxe and Watson, 1994; Fig. 3), two of them within site (ORS4 and ORS6) and the other two including two sites each. Fold-tests show a syn-folding (IL–IL7) and a non-conclusive but likely post-folding magnetizations (Fig. 3). Two of the non-conclusive fold-tests show better clustering in geographical coordinates than after correction (Fig. 3; ORS4 and ORS6), the last one is not affected by unfolding.

We have separated the samples collected to the north and south of the Killarney–Mallow Fault to investigate the possible effects in the obtained paleomagnetic directions depending on the contrasting structural styles at both sides of the fault (Fig. 4; Table 1). Site means (Fig. 4A) tend to support more similarities in geographical coordinates than in tilt corrected. Total averages from north and south of Killarney–Mallow fault show an A quality common true mean direction (CMTD; McFadden and McElhinny, 1990) in geographic coordinates and negative CMTD in tilt corrected coordinates. Additionally A95 is in between $A95_{max}$ and $A95_{min}$ in both cases suggesting that datasets are not affected by large sources of scatter rather than PSV. An overall tilt test (Fig. 4C) shows a maximum eigen vector at ca. 25% of untilting.

We have also calculated a total average of the collected samples (Table 1; Fig. 5A) to obtain a reliable pole. The resulting pole (pole lat/long = 32/133) shows better grouping ($K = 18.5$) in geographical coordinates with an $A95(1.9) < A95_{max}$ (2.1; Table 1) than tectonic coordinates ($K = 12.5$) with $A95(2.4) > A95_{max}(2.3)$. Additionally, in geographical coordinates only 3% of the samples do not pass a 45° cutoff, whereas after tilt correction 13% of the samples are rejected.

Orogenic bends are classified based on the kinematics of their development of curvature (Weil and Sussman, 2004; Johnston et al., 2013). Correlations between changes in the structural grain and paleomagnetic directions or rock fabrics are evaluated using an orocline test (Eldredge et al., 1985; Yonkee and Weil, 2010) which distinguishes two end-members: 1) primary bends, showing a slope ($m$) = 0 and 2) secondary oroclines, with $m = 1$. Intermediate relations ($0 < m < 1$) are known as progressive oroclines. We have performed an oroclinal test following the method described in Yonkee and Weil (2010; Fig. 5) combining our data from southern Ireland with the orocline test from the Cantabrian Orocline (Weil et al., 2013; Fig. 6) in order to check the fit of Ireland in

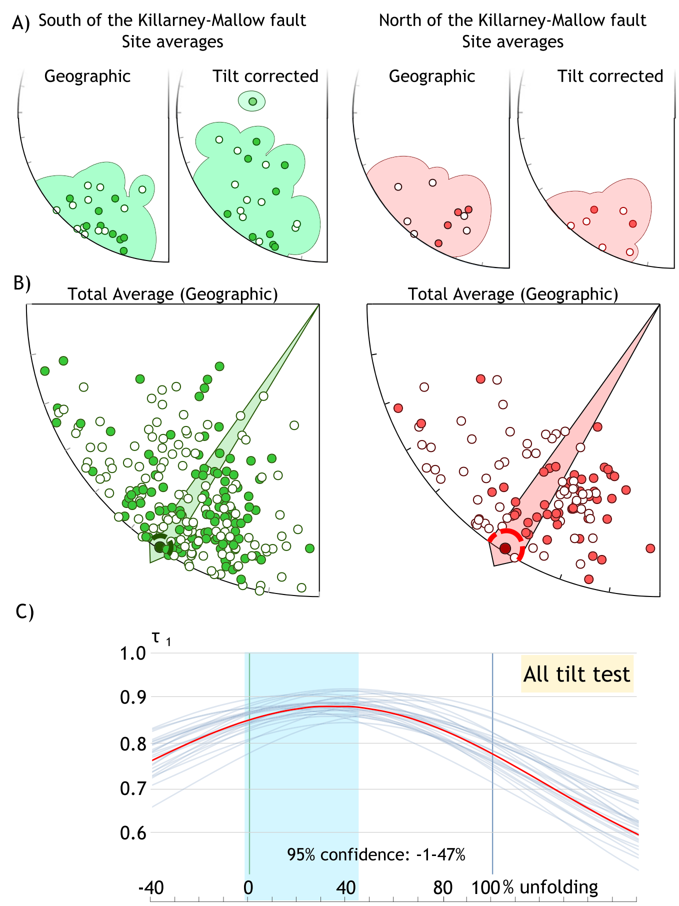


**Fig. 4.** A) In green, means of sites situated to the south of the Killarney Fault showing the A95 envelope projected (in geographic and tilt corrected coordinates). In red, site means of the collected samples to the north of the Killarney Fault (in geographic and tilt corrected coordinates). B) Total average of those sites in Geographic coordinates, again green for samples collected to the south and red to the north of Killarney Fault. C) Tilt test considering all samples showing better clustering at a 25%. It reinforces our interpretation of a syn- to post-folding remagnetization. (For interpretation of the references to color in this figure legend, the reader is referred to the web version of this article.)

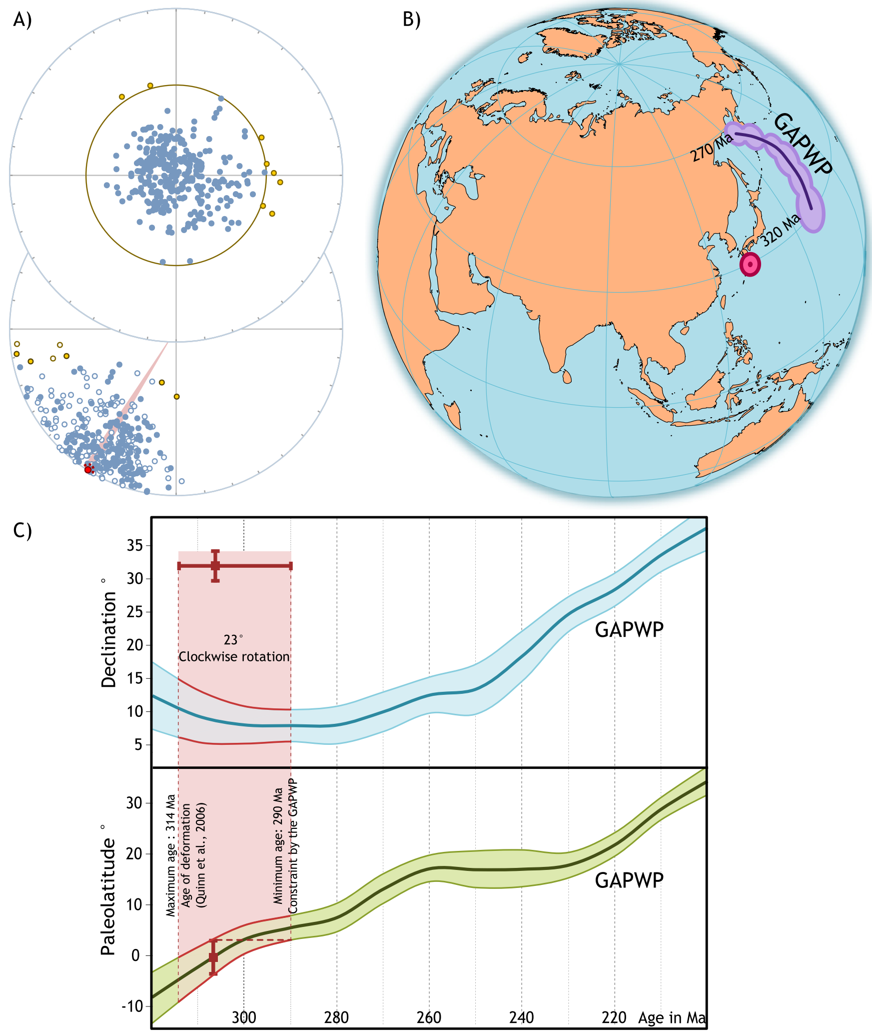


**Fig. 5.** Pole for southern Ireland during the Late Carboniferous. A) VGP and equal area projections showing a fixed 45° cut-off. Solid points are lower hemisphere and empty upper hemisphere projections. Yellow points are discarded. B) South Ireland Pole vs. GAPWP from Torsvik et al. (2012). Note the coincidence in latitude and the difference in longitude. C) Pole of South Ireland vs. GAPWP showing the obtained declination and paleolatitude vs. the expected ones. (For interpretation of the references to color in this figure legend, the reader is referred to the web version of this article.)

the Cantabrian Orocline, all data together fit with a line of slope equal to $0.94 \pm 0.03$.

## 4. Discussion

### *4.1. Paleomagnetism of southern Ireland: timing and style*

Fold- and tilt-tests show not fully conclusive syn- to post-folding magnetizations (Figs. 3 and 4C). Despite the difference in age of the samples (Early Devonian to Late Carboniferous), we documented consistent low latitudes and no changes in polarity for the time of magnetization of the studied rocks. The occurrence of a single polarity indicates that rocks were magnetized during a single magnetic chron, meaning that either the process was very quick or occurred during a single superchron. Relatively shallow inclinations constrain the magnetization to a short period of time since it records no changes in latitude as it is expected for the Late Paleozoic (Torsvik et al., 2012). Combining the latter with the occurrence of a single polarity and syn- to post-folding magnetizations constrained the magnetization to the period associated with Variscan folding (314–302 Ma; Quinn et al., 2005) and the Kiaman reverse superchron (310–265 Ma; Langereis et al., 2010).

We have sampled in two structurally different areas, (i) the internally more deformed units situated to the south and (ii) the more gently folded units to the north of Killarney–Mallow Fault; and in different lithologies: limestones and silt to sandstones. When comparing results from the two structural units we found a CTMD of A quality (meaning the same direction), before any correction. Meaning that in average both South and North of Killarney–Mallow Fault have rotated the same ∼25° clockwise. Additionally, we identified no major local rotations due to structural complexities in any of the sampled localities and areas.

### *4.2. Late carboniferous pole for southern Ireland*

Paleomagnetic poles are commonly estimated from sets of paleomagnetic directions. Paleosecular variation (PSV) of the magnetic field happens in geologically short timescales and leads to a scatter of the obtained directions in the distribution of the virtual geomagnetic poles (Deenen et al., 2011). For tectonic purposes, paleomagnetic sampling is commonly carried out at multiple sites to be able to recognize local rotations. Averaging of PSV therefore requires obtaining a sufficiently large number of individual spot readings over a sufficiently long time interval, but short enough to avoid the effect of plate motions. It has been common in paleomagnetism to average site means to obtain finite rotations and poles. This practice can be problematical: sites with unequal numbers of samples are given equal importance and the statistics of

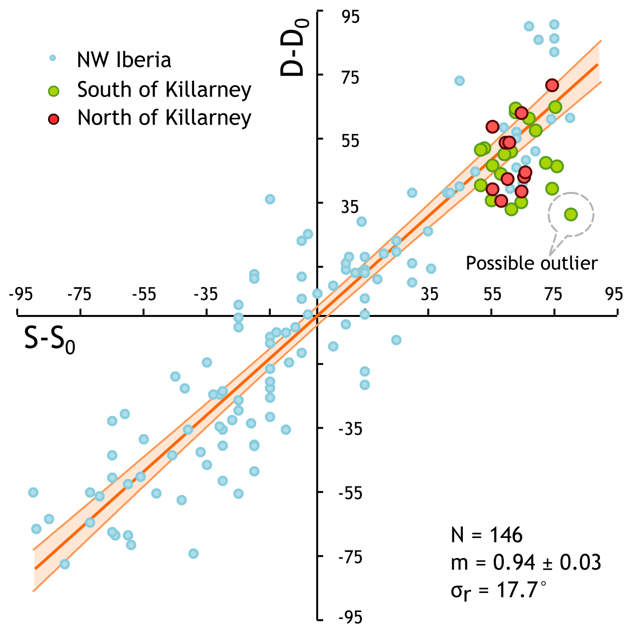


**Fig. 6.** Paleomagnetic strike test for data from the Cantabrian Orocline (Weil et al., 2013) including the results from southern Ireland and the statistics of data altogether including southern Ireland and NW Iberia. In green results from the south of the Killarney Fault and in red the ones coming from the north of this structure. Best-fit slopes ($m$), number of sites ($N$), uncertainty of the slope (± corresponding with $2\sigma$), and standard deviation of residuals ($\sigma_r$) are given. (For interpretation of the references to color in this figure legend, the reader is referred to the web version of this article.)

each site mean are not taken into account. Averaging all individual directions into a tectonic unit locality allows for a better overall assessment if the sampled scatter is consistent with PSV and the effect of other processes as local rotations that contribute to the scatter.

We have calculated a pole for southern Ireland considering all the analyzed samples (Fig. 5A). The resulting average ($D = 212.3°$, $I = 0.5°$; pole to lat/long = 32°/132°; Table 1) with a VGP circular distribution (Fig. 5A). When using the tilt corrected values the direction obtained is very similar (214/−5.1), but shows less clustering and the A95 becomes larger than $A95_{max}$ indicating an additional source of scatter, in this case tilt correction. We consider the pole in geographic coordinates as the best approximation since we could not characterize the optimum percentage of tilt correction necessary per site.

The maximum age of the pole is constrained by folding time (from 314–302 Ma; Quinn et al., 2005). Its minimum age is constrained by the inclination of the pole $-0.5° \pm 1.9°$ which following the GAPWP (Torsvik et al., 2012) confines the minimum possible age of the magnetization to 290 Ma. We used the stable Europe curve corrected for the latitude of Macroom, county Cork (lat: 51.9°; long: 8.96°; Fig. 5). We assigned the pole an age of $307 \pm 6$ Ma. At this time, the paleolatitude obtained for southern Ireland (−0.25°) fits excellently with the expected paleolatitude in South Ireland in the GAPWP (−0.5°). Despite the agreement in paleolatitude, the obtained declination shows ca. 25° clockwise rotation from that extracted from GAPW (Fig. 5B and C). Mac Niocaill (2000) documented a similar clockwise rotation in Silurian rocks of the Dingle Peninsula, although he considered the rotation to be either a rotation of Avalonia during the closure of the Iapetus ocean or more 'local' rotations. It is known that Ireland follows the stable Europe GAPWP from at least 290 Ma (e.g. Pannalal et al., 2008). Our results from southern Ireland show that the rotation is regional, affecting at least all South Ireland and that it happened in a short interval from 314 to 290 Ma. This is long after the closure of Iapetus and therefore it is not a product of the Caledonian collision.

### 4.3. Oroclinal bending

The orocline test evaluates the relationship between variations in regional structural trend and the orientations of given geologic fabric elements (e.g., paleomagnetic declinations, fractures, cleavage, veins, lineations, etc.). Southern Ireland shows a curvature of ca. 25° which is very close to the limit of resolution of paleomagnetism considering that: 1) Sites of 25 samples show errors in declinations ($\Delta D$) up to ±5 (Deenen et al., 2011) and 2) estimating the strike of that orogen may involve errors up to ±8° (Yonkee and Weil, 2010). A curvature like the observed in South Ireland (∼25°) would require an extraordinary amount of sites to get a reliable result (768 sites, following Yonkee and Weil, 2010). However, including our Irish data to the Cantabrian Orocline data is indeed a good method to evaluate the involvement of southern Ireland into the orocline formation. We have performed an oroclinal test following the method described in Yonkee and Weil (2010; Fig. 6). In order to properly compare the orientations in Iberia and in Ireland we have rotated the strike of the Variscan orogeny 35° clockwise in Iberia back to a pre-opening of the Biscay Bay (Gong et al., 2008). The southern Ireland data fit very well with the Cantabrian Orocline and significantly add to the scarcer data-set in its northern branch. All data together yield a slope of $0.94 \pm 0.03$ (Fig. 6) indicating a secondary origin for this orocline.

### 4.4. The greater Cantabrian Orocline: implications and challenges

The Cantabrian Orocline, traditionally known as Ibero-Armorican Arc (e.g. Ries and Shackleton, 1976), has been defined as a convex to the northwest curved orogenic system that weaves through the Iberian and Armorican Massifs following the geometrical changes in the structural trend of thrusts and folds that formed during the Variscan orogeny (e.g. Ribeiro et al., 2007). Structural and paleomagnetic constraints previously discussed indicate that the Cantabrian Orocline is a large-scale feature including Iberia and part of France (Gutiérrez-Alonso et al., 2008; Weil et al., 2013; Pastor-Galán et al., 2015) that formed in the latest Carboniferous (Fig. 7) (Pastor-Galán et al., 2011; Weil et al., 2013) during the final stages of the formation of Pangea (Gutiérrez-Alonso et al., 2008; Pastor-Galán et al., 2015).

The Avalonian microplate assemblage, including southern Ireland and the South Portuguese Zone (SW Iberia), accreted to Laurentia and Baltica forming Laurussia in the middle to late Silurian (e.g. Mac Niocaill, 2000; Murphy et al., 2006). These areas made up the Laurussian southern margin until the Gondwana–Laurentia collision that led to the final assembly of Pangea during the late Carboniferous (Nance et al., 2010). Southern Ireland displays a geometrical fit with the Iberian Variscan Orogen, once Iberia is restored to a pre-Bay of Biscay opening (Fig. 1; Gong et al., 2008). Our results show that vertical axis rotations in southern Ireland and Iberia are synchronous (Pastor-Galán et al., 2011, 2014) and kinematically consistent, showing clockwise rotations in the north and counterclockwise in the south. This observation strongly suggests the participation of a large segment of Avalonia in Cantabrian oroclinal buckling involving, at least, southern Ireland and the South Portuguese Zone (Fig. 7) suggesting the formation of a Late Variscan orocline affecting both Gondwana and Laurussia margins: a Greater Cantabrian Orocline.

Fig. 7 sketches a plausible kinematic explanation for the formation of a Greater Cantabrian Orocline. In the latest stages of the Variscan orogeny, ca. 310 Ma (Fig. 7A), a change in the regional stress field – from E–W to N–S in present day coordinates – would lead to along strike buckling of the Variscan

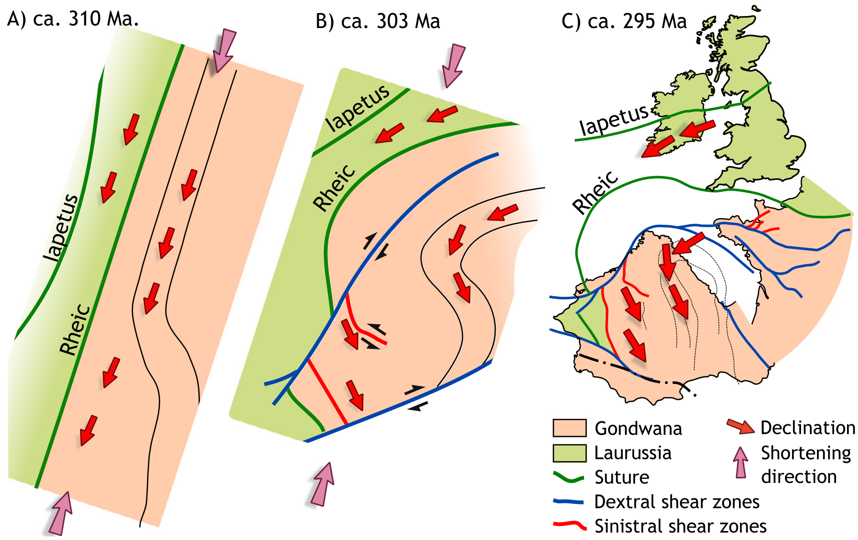


**Fig. 7.** Tectonic evolution of the Greater Cantabrian Orocline during Upper Pennsylvanian times. A) Latest stage of Western Europe Variscan Belt development, highlighted by a nearly linear orogen in which paleomagnetic directions are shown. B) Buckling of the Variscan orogen related to a change in the regional stress-field. C) Final architecture of the Variscan orogen before the opening of the Biscay Bay. See text for further details.

orogen within the recently amalgamated Pangea supercontinent (Gutiérrez-Alonso et al., 2008; Pastor-Galán et al., 2015) producing the Greater Cantabrian Orocline that in its outermost part describes a C trace from southern Ireland to the South-Portuguese Zone (Fig. 7C).

Although kinematic observations indicate a secondary origin for the Cantabrian Orocline, it remains unclear as to what possible mechanisms caused the necessary far-field stress change to form such a large, plate-scale structure that seems to involve the entire lithosphere (Gutiérrez-Alonso et al., 2011b; Pastor-Galán et al., 2012). Several models have been proposed including: (i) the self-subduction of Pangea (Gutiérrez-Alonso et al., 2008), (ii) buckling of a ribbon continent between Laurussia and Gondwana during the final amalgamation of Pangea (Johnston and Gutierrez-Alonso, 2010, and Weil et al., 2010), (iii) a continental-scale post-Variscan dextral shear zone (Martínez Catalán, 2011); and (iv) rotation of Gondwana producing a buttress effect that buckles the Variscan Orogen (Pastor-Galán et al., 2015). A Greater Cantabrian Orocline, including southern Ireland into it, surpass its traditional limits: the crustal scale shear zones in the Variscan hinterland (Weil et al., 2013; Gutiérrez-Alonso et al., 2015) and the Rheic Ocean suture (Ribeiro et al., 2007; Weil et al., 2010; Martínez Catalán, 2011). The formation of Greater Cantabrian Orocline would require shortening and extension (>1000 km) in a period of time of <15 m.y. (Pastor-Galán et al., 2012, 2014) as well as major crustal detachments and/or subduction zones yet to be described. A formation of such structure questions the mechanisms proposed for the formation of the Cantabrian Orocline and challenges most of the existing Paleozoic global reconstructions (e.g. Stampfli et al., 2013; Domeier and Torsvik, 2014). It also adds an interrogation to one of the main assumptions in plate tectonics, plate rigidity (Gordon, 1998; Torsvik et al., 2012).

## 5. Conclusions

The paleomagnetic results presented in this study indicate a clockwise vertical-axis rotation of ∼25° in southern Ireland during Late Carboniferous and earliest Permian. Rotation occurred approximately coeval to deformation and pervasive remagnetization. The rotation of southern Ireland happened synchronously and fits geometrically with the development of the Cantabrian Orocline, in north-west Iberia. We conclude that southern Ireland is part of a Greater Cantabrian Orocline that affected two continental margins Gondwana and Laurussia.

## Acknowledgements

We want to thank Mark Dekkers for discussion and useful comments. Brenton Fairey, Thomas Groenewegen and Aidan Kerrison are thanked for laboratory assistance. This research is funded by the Netherlands Organization for Scientific Research (NWO). We are in debt with the insights, discussion and constructive comments provided by Rob van der Voo and Emilio Pueyo. DPG would like to thank a postdoctoral grant from ISES (project no. WA.146101.2.656). This paper is a contribution to IUGS-UNESCO's IGCP projects no. 574 "Bending and Bent Orogens, and Continental Ribbons", no. 597 "Amalgamation and Breakup of Pangaea" and no. 648 "Supercontinent Cycles & Global Geodynamics".

## Appendix A. Supplementary material

Supplementary material related to this article can be found online at http://dx.doi.org/10.1016/j.epsl.2015.10.019. These data include the Google map of the most important areas described in this article.

## References

Allmendinger, R.W., Smalley, R., Bevis, M., Caprio, H., Brooks, B., 2005. Bending the Bolivian orocline in real time. Geology 33, 905–908. http://dx.doi.org/10.1130/G21779.1.

Deenen, M.H.L., Langereis, C.G., van Hinsbergen, D.J.J., Biggin, A.J., 2011. Geomagnetic secular variation and the statistics of palaeomagnetic directions. Geophys. J. Int. 186, 509–520. http://dx.doi.org/10.1111/j.1365-246X.2011.05050.x.

Domeier, M., Torsvik, T.H., 2014. Plate tectonics in the late Paleozoic. Geosci. Front. 5, 303–350. http://dx.doi.org/10.1016/j.gsf.2014.01.002.

Eldredge, S., Bachtadse, V., Van Der Voo, R., 1985. Paleomagnetism and the orocline hypothesis. Tectonophysics 119, 153–179. http://dx.doi.org/10.1016/0040-1951(85)90037-X.

Fernández-Suárez, J., Gutiérrez-Alonso, G., Pastor-Galán, D., Hofmann, M., Murphy, J.B., Linnemann, U., 2014. The Ediacaran–Early Cambrian detrital zircon record of NW Iberia: possible sources and paleogeographic constraints. Int. J. Earth Sci. 103, 1335–1357. http://dx.doi.org/10.1007/s00531-013-0923-3.

Gong, Z., Langereis, C.G., Mullender, T.A.T., 2008. The rotation of Iberia during the Aptian and the opening of the Bay of Biscay. Earth Planet. Sci. Lett. 273, 80–93.

Gordon, R.G., 1998. The plate tectonic approximation: plate nonrigidity, diffuse plate boundaries, and global plate reconstructions. Annu. Rev. Earth Planet. Sci. 26, 615–642. http://dx.doi.org/10.1146/annurev.earth.26.1.615.

Gutiérrez-Alonso, G., Collins, A.S., Fernández-Suárez, J., Pastor-Galán, D., González-Clavijo, E., Jourdan, F., Weil, A.B., Johnston, S.T., 2015. Dating of lithospheric buckling: $^{40}Ar/^{39}Ar$ ages of syn-orocline strike-slip shear zones in northwestern Iberia. Tectonophysics. http://dx.doi.org/10.1016/j.tecto.2014.12.009.

Gutiérrez-Alonso, G., Fernández-Suárez, J., Jeffries, T.E., Johnston, S.T., Pastor-Galán, D., Murphy, J.B., Franco, M.P., Gonzalo, J.C., 2011a. Diachronous post-orogenic magmatism within a developing orocline in Iberia, European Variscides. Tectonics 30. http://dx.doi.org/10.1029/2010TC002845, 17 pp.

Gutiérrez-Alonso, G., Fernández-Suárez, J., Weil, A.B., Murphy, J.B., Nance, R.D., Corfu, F., Johnston, S.T., 2008. Self-subduction of the Pangaean global plate. Nat. Geosci. 1, 549–553.

Gutiérrez-Alonso, G., Johnston, S.T., Weil, A.B., Pastor-Galán, D., Fernández-Suárez, J., 2012. Buckling an orogen: the Cantabrian orocline. GSA Today 22, 4–9.

Gutiérrez-Alonso, G., Murphy, J.B., Fernández-Suárez, J., Weil, A.B., Franco, M.P., Gonzalo, J.C., 2011b. Lithospheric delamination in the core of Pangea: Sm–Nd insights from the Iberian mantle. Geology 39, 155–158. http://dx.doi.org/10.1130/G31468.1.

Johnston, S.T., 2001. The Great Alaskan Terrane Wreck: reconciliation of paleomagnetic and geological data in the northern Cordillera. Earth Planet. Sci. Lett. 193, 259–272.

Johnston, S.T., Gutierrez-Alonso, G., 2010. The North American Cordillera and West European Variscides: contrasting interpretations of similar mountain systems. Gondwana Res. 17, 516–525. http://dx.doi.org/10.1016/j.gr.2009.11.006.

Johnston, S.T., Weil, A.B., Gutierrez-Alonso, G., 2013. Oroclines: thick and thin. Geol. Soc. Am. Bull. 125, 643–663. http://dx.doi.org/10.1130/B30765.1.

Kirschvink, J.L., 1980. The least-squares line and plane and the analysis of palaeomagnetic data. Geophys. J. Int. 62, 699–718. http://dx.doi.org/10.1111/j.1365-246X.1980.tb02601.x.

Langereis, C.G., Krijgsman, W., Muttoni, G., Menning, M., 2010. Magnetostratigraphy – concepts, definitions, and applications. Newsl. Stratigr. 43, 207–233. http://dx.doi.org/10.1127/0078-0421/2010/0043-0207.

MacCarthy, I.A.J., 1990. Alluvial sedimentation patterns in the Munster Basin, Ireland. Sedimentology 37, 685–712.

Mac Niocaill, C., 2000. A new Silurian palaeolatitude for eastern Avalonia and evidence for crustal rotations in the Avalonian margin of southwestern Ireland. Geophys. J. Int. 141, 661–671. http://dx.doi.org/10.1046/j.1365-246x.2000.00101.x.

Martínez Catalán, J.R., 2011. Are the oroclines of the Variscan belt related to late Variscan strike-slip tectonics? Terra Nova 23, 241–247. http://dx.doi.org/10.1111/j.1365-3121.2011.01005.x.

McFadden, P.L., McElhinny, M.W., 1990. Classification of the reversal test in palaeomagnetism. Geophys. J. Int. 103, 725–729. http://dx.doi.org/10.1111/j.1365-246X.1990.tb05683.x.

Meere, P.A., 1995. The structural evolution of the western Irish Variscides: an example of obstacle tectonics? Tectonophysics 246, 97–112.

Murphy, J.B., Gutierrez-Alonso, G., Nance, R.D., Fernandez-Suarez, J., Keppie, J.D., Quesada, C., Strachan, R.A., Dostal, J., 2006. Origin of the Rheic Ocean: rifting along a Neoproterozoic suture? Geology 34, 325–328. http://dx.doi.org/10.1130/G22068.1.

Nance, R.D., Gutiérrez-Alonso, G., Keppie, J.D., Linnemann, U., Murphy, J.B., Quesada, C., Strachan, R.A., Woodcock, N.H., 2010. Evolution of the Rheic Ocean. Gondwana Res. 17, 194–222. http://dx.doi.org/10.1016/j.gr.2009.08.001.

Pannalal, S.J., Symons, D.T.A., Sangster, D.F., 2008. Palaeomagnetic evidence of a Variscan age for the epigenetic Galmoy zinc-lead deposit, Ireland. Terra Nova 20, 385–393. http://dx.doi.org/10.1111/j.1365-3121.2008.00832.x.

Pastor-Galán, D., Groenewegen, T., Brouwer, D., Krijgsman, W., Dekkers, M.J., 2015. One or two oroclines in the Variscan orogen of Iberia? Implications for Pangea amalgamation. Geology 43, 527–530. http://dx.doi.org/10.1130/G36701.1.

Pastor-Galán, D., Gutiérrez-Alonso, G., Fernández-Suárez, J., Murphy, J.B., Nieto, F., 2013a. Tectonic evolution of NW Iberia during the Paleozoic inferred from the geochemical record of detrital rocks in the Cantabrian Zone. Lithos 182–183, 211–228. http://dx.doi.org/10.1016/j.lithos.2013.09.007.

Pastor-Galán, D., Gutiérrez-Alonso, G., Murphy, J.B., Fernández-Suárez, J., Hofmann, M., Linnemann, U., 2013b. Provenance analysis of the Paleozoic sequences of the northern Gondwana margin in NW Iberia: passive margin to Variscan collision and orocline development. Gondwana Res. 23, 1089–1103. http://dx.doi.org/10.1016/j.gr.2012.06.015.

Pastor-Galán, D., Gutiérrez-Alonso, G., Weil, A.B., 2011. Orocline timing through joint analysis: insights from the Ibero-Armorican Arc. Tectonophysics 507, 31–46. http://dx.doi.org/10.1016/j.tecto.2011.05.005.

Pastor-Galán, D., Gutierrez-Alonso, G., Zulauf, G., Zanella, F., 2012. Analogue modeling of lithospheric-scale orocline buckling: constraints on the evolution of the Iberian-Armorican Arc. Geol. Soc. Am. Bull. 124, 1293–1309. http://dx.doi.org/10.1130/B30640.1.

Pastor-Galán, D., Martín-Merino, G., Corrochano, D., 2014. Timing and structural evolution in the limb of an orocline: the Pisuerga–Carrión Unit (southern limb of the Cantabrian Orocline, NW Spain). Tectonophysics 622, 110–121. http://dx.doi.org/10.1016/j.tecto.2014.03.004.

Price, C.A., Todd, S.P., 1988. A model for the development of the Irish Variscides. J. Geol. Soc. (Lond.) 145, 935–939.

Quinn, D., Meere, P.A., Wartho, J.A., 2005. A chronology of foreland deformation: ultra-violet laser Ar-40/Ar-39 dating of syn/late-orogenic intrusions from the Variscides of southwest Ireland. J. Struct. Geol. 27, 1413–1425.

Ramón, M.J., Pueyo, E.L., 2012. Automatic calculation of demagnetization intervals; a new approach based on the virtual directions method and comparison with the linearity spectrum analysis. In: VIII Congreso Geológico de España. Geotemas 13, 1180–1183.

Ribeiro, A., Munhá, J., Dias, R., Mateus, A., Pereira, E., Ribeiro, L., Fonseca, P., Araújo, A., Oliveira, T., Romão, J., Chaminé, H., Coke, C., Pedro, J., 2007. Geodynamic evolution of the SW Europe Variscides. Tectonics 26, 24. http://dx.doi.org/10.1029/2006TC002058.

Ries, A.C., Shackleton, R.M., 1976. Patterns of strain variation in arcuate fold belts. Philos. Trans. R. Soc. Lond. Ser. A, Math. Phys. Sci. 283, 281–288.

Rosenbaum, G., 2014. Geodynamics of oroclinal bending: insights from the Mediterranean. J. Geodyn. 82, 5–15. http://dx.doi.org/10.1016/j.jog.2014.05.002.

Shaw, J., Gutierrez-Alonso, G., Johnston, S.T., Galan, D.P., Pastor Galan, D., 2014. Provenance variability along the Early Ordovician north Gondwana margin: paleogeographic and tectonic implications of U–Pb detrital zircon ages from the Armorican Quartzite of the Iberian Variscan belt. Geol. Soc. Am. Bull. 126, 702–719. http://dx.doi.org/10.1130/B30935.1.

Shaw, J., Johnston, S.T., Gutiérrez-Alonso, G., Weil, A.B., 2012. Oroclines of the Variscan orogen of Iberia: paleocurrent analysis and paleogeographic implications. Earth Planet. Sci. Lett. 329–330, 60–70. http://dx.doi.org/10.1016/j.epsl.2012.02.014.

Stampfli, G.M., Hochard, C., Vérard, C., Wilhem, C., VonRaumer, J., 2013. The formation of Pangea. Tectonophysics 593, 1–19. http://dx.doi.org/10.1016/j.tecto.2013.02.037.

Tauxe, L., Watson, G.S., 1994. The fold test: an eigen analysis approach. Earth Planet. Sci. Lett. 122, 331–341. http://dx.doi.org/10.1016/0012-821X(94)90006-X.

Torsvik, T.H., Van der Voo, R., Preeden, U., Mac Niocaill, C., Steinberger, B., Doubrovine, P.V., van Hinsbergen, D.J.J., Domeier, M., Gaina, C., Tohver, E., Meert, J.G., McCausland, P.J., Cocks, L.R.M., 2012. Phanerozoic polar wander, palaeogeography and dynamics. Earth-Sci. Rev. 114, 325–368. http://dx.doi.org/10.1016/j.earscirev.2012.06.007.

Weil, A.B., Gutiérrez-Alonso, G., Johnston, S.T., Pastor-Galán, D., 2013. Kinematic constraints on buckling a lithospheric-scale orocline along the northern margin of Gondwana: a geologic synthesis. Tectonophysics 582, 25–49. http://dx.doi.org/10.1016/j.tecto.2012.10.006.

Weil, A.B., Gutiérrez-Alonso, G., Conan, J., 2010. New time constraints on lithospheric-scale oroclinal bending of the Ibero-Armorican Arc: a paleomagnetic study of earliest Permian rocks from Iberia. J. Geol. Soc. (Lond.) 167, 17. http://dx.doi.org/10.1144/0016-76492009-002.

Weil, A.B., Sussman, A.J., 2004. Classifying curved orogens based on timing relationships between structural development and vertical-axis rotations. In: Sussman, A.J., Weil, A.B. (Eds.), Geological Society of America, pp. 1–16.

Williams, E.A., Bamford, M.L.F., Cooper, M.A., Edwards, H.E., Ford, M., Grant, G.G., MacCarthy, I.A.J., McAfee, A.M., O'Sullivan, M.J., 1989. Tectonic controls and sedimentary response in the Devonian–Carboniferous Munster Basin, southwest Ireland. In: Arturton, R.S., Gutteridge, P., Nolan, S.C. (Eds.), The Role of Tectonics in Devonian and Carboniferous Sedimentation in the British Isles. In: Spec. Publ. Yorkshire Geol. Soc., vol. 6, pp. 123–141.

Williams, E.A., 2000. Flexural cantilever models of extensional subsidence in the Munster Basin (SW Ireland) and Old Red Sandstone dispersal systems. In: Friend, P.F., Williams, B.P.J. (Eds.), New Perspectives on the Old Red Sandstone. In: Geol. Soc. (Lond.) Spec. Publ., vol. 180, pp. 239–268.

Yonkee, A., Weil, A.B., 2010. Quantifying vertical axis rotation in curved orogens: correlating multiple data sets with a refined weighted least squares strike test. Tectonics 29, 31. http://dx.doi.org/10.1029/2008TC002312.

Zijderveld, J.D.A., 1967. A.C. demagnetization of rocks: analysis of results. In: Collinson, D., Creer, K., Runcorn, S. (Eds.), Methods in Paleomagnetism. Elsevier, Amsterdam, pp. 254–286.